Journal of New Technology and Materials (JNTM)
J. New Technol. Mater.
Vol. 08, N°01 (2018)48-57

OEB Univ. Publish. Co.

Numerical investigation of three-dimensional heat transfer and natural convection in the sapphire melt for Czochralski growth process

H. Azoui[a], N. Soltani[b] and D. Bahloul[a]

[a]*PRIMALAB Laboratory, Department of Physics, University of Batna1, 1 rue Chahid Boukhlouf Mohamed El-Hadi, 05000 Batna, Algeria.*
[b]*LESEI Laboratory, Department of Mechanical Engineering, University of Batna 2, 53 Route de Constantine. Fésdis, Batna 05078, Algeria.*

Corresponding author: email: anhananе@gmail.com

Received date: Mar. 29, 2018; revised date: Apr. 20, 2018; accepted date: Apr. 24, 2018

Abstract

A three-dimensional numerical study of the convection heat transfer in a simulated Czochralski system is conducted .In this work, the numerical investigation were performed to analyze the free convection in the Czochralski crucible and the temperature fluctuations(thermal instabilities) just below the melt-crystal interface. We used the Finite Volume Method in cylindrical coordinates and the Fast Fourier Transform method for study the free convection, the temperature fluctuations 2 mm near the interface by taking into account the case of non-rotating crystal. In this study the heat transfer, thermal instabilities, melt natural convection, radiative heat transfer, Marangoni convection were conducted for Al_2O_3 melt in the crucible. Our objective is to show the fluctuations of temperature just below the interface by taking into account the effect of Rayleigh number for determining the crucible heating temperature value, and display the problem and his solution of the natural convection in the Czochralski crucible.

Keywords: Natural convection, Heat transfer, Sapphire, Czochralski method, Shaped crystals, Thermal instabilities, Crystal growth.;

1. Introduction

In a number of modern high-technology applications, sapphire single crystals are used widely in several systems. Sapphire (Al_2O_3) is a very important material because of its specific structure and its exceptional optical, thermal and electrical properties, [1]. In different and various systems and applications, Al_2O_3 is used widely in optical systems, needles for laser therapy and medical power delivery systems watch windows, cellular phone glasses, optical fibers, and in wave guides for surgery [2, 3]. We also cite the use of this material as a optical window material and, filter material for thermal neutron beams and a substrate material for the epitaxial deposition [4]. Many crystal growth methods have been used to grow this material. Among these techniques the Czochralski (Cz) is an excellent commercial process for growing larger, high optical-quality sapphire crystals with fewer defects. The temperature distribution and convection of molten sapphire during the manufacturing process influence largely on the properties and on the growth behavior of sapphire crystals.

Different types of heat transfer mechanism coexist in the Czochralski growth setup which are convection, conduction and radiation within the melt, conduction and radiation within the grown crystal, gas convection and radiative heat exchange between the exposed surfaces. Several researchers studied the convective heat transfer such as melt hydrodynamics [5–8], melt and gas flow pattern [9–11] and influence of the melt convection mode on the shape of the crystal-melt interface with respect to physical and geometrical parameters of the melt and growth configuration [12–18]. Detailed analyses of the interface shape, transition and its inversion during growth of high melting oxide crystals can be found in several reports [19, 20]. In the Czochralski process the melt convection is mainly induced by natural convection due to the buoyancy and surface tension effect, forced convection due to the crystal and crucible rotation and electromagnetically induced convection if the electromagnetic field is applied. In these convections, the melt natural convection cannot be eliminated and is strongly influenced by temperature distribution along the crucible wall. In this work the melt natural convection, heat transfer, temperature fluctuations (thermal instabilities), were conducted for Al_2O_3 melt in the Cz crucible. The finite volume method and the Fast Fourier Transform are used for study the temperature fluctuations near the crystal/liquid interface. Our objective is to reduce the fluctuations of temperature just near the interface by taking into account the case of non-rotating seed. The

heating temperature of the crucible walls is calculated by studying the effect of Rayleigh number on the temperature fluctuations in the crucible. In this analysis, we consider that the crystal-melt interface and the melt free surface are flat; the crystal and crucible are not rotated.

In the next section we present the modeling growth system using the Czochralski technique. In Section 3 we present the mathematical formulation of our model that is the governing equations, the boundary conditions and the numerical scheme used in our simulations. Section 4 is devoted to the results and discussion, followed by conclusions in section 5.

2. Model of Czochralski growth system

The model for Czochralski crystal growth furnace is schematically illustrated in Fig. 1. In this process, the melt (sapphire) is placed in a cylindrical crucible (see fig.2), located in a furnace.

In the sapphire case, the crucible walls are heated above the melting temperature $\boldsymbol{T_{crucible} \approx 2373\ K}$ by a radiofrequency inductive heating system. The production of a cylindrical crystal due to the phase change phenomena with connection between the liquid and the sapphire seed at the crystal-melt interface. The crystal produced is vertically pulled out of the melt as shown in the schematic diagram below:

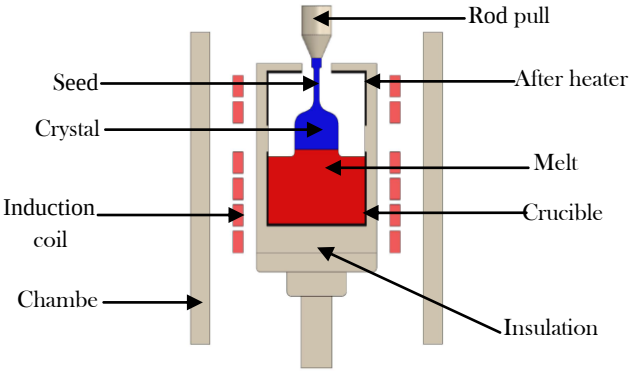

Figure 1. Schematic model of the inductively heated Czochralski furnace.

Fig. 2 shows the crucible geometry which depends on the Czochralski technique. In our simulation we use a crucible with a height of 0.1 m, a diameter of 0.1 m and an interface with a diameter of 0.03 m. The melt sapphire is presented with the red color, the melt - crystal interface displayed with the blue color, the green color presents the sapphire melt free surface.

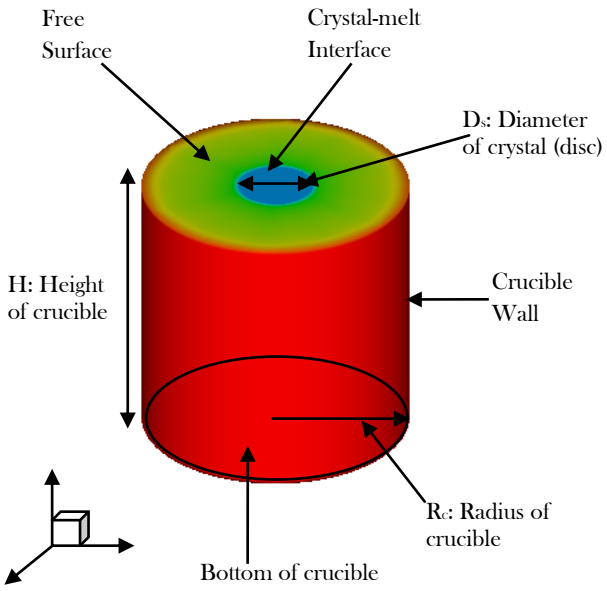

Figure 2. Schematic diagram of the Czochralski crucible.

2.1. Mathematical model

The fundamental equations consist the continuity equation, the momentum equation and the energy equation. The melt is assumed incompressible and Newtonian, while the flow is laminar. In a pure sapphire melt, free convection, Marangoni convection (Surface tension driven flow), and radiation are to be considered. These flows are satisfactorily expressed by the unsteady state Navier-Stokes equations with Boussinesq approximation and the continuity equation in cylindrical coordinates (r, θ, z). The flow, the heat transfer are modeled by the following differential equations:

Equation of radial component of the momentum:

$$\frac{\partial u}{\partial t}+u\frac{\partial u}{\partial r}+\frac{v}{r}\frac{\partial u}{\partial \theta}-\frac{v^2}{r}+w\frac{\partial u}{\partial z}=-\frac{1}{\rho_m}\frac{\partial P}{\partial r}+$$
$$\nu\left(\frac{1}{r}\frac{\partial}{\partial r}\left(r\frac{\partial u}{\partial r}\right)-\frac{u}{r^2}+\frac{1}{r^2}\frac{\partial^2 u}{\partial \theta^2}-\frac{2}{r^2}\frac{\partial v}{\partial \theta}+\frac{\partial^2 u}{\partial z^2}\right)$$
$$+\frac{1}{\rho_m}(\rho g_r) \qquad (1)$$

Equation of azimuthally component of the momentum

$$\frac{\partial v}{\partial t}+u\frac{\partial v}{\partial r}+\frac{v}{r}\frac{\partial v}{\partial \theta}-\frac{uv}{r}+w\frac{\partial v}{\partial z}=-\frac{1}{\rho_m}\frac{1}{r}\frac{\partial P}{\partial \theta}+$$
$$\nu\left(\frac{1}{r}\frac{\partial}{\partial r}\left(r\frac{\partial v}{\partial r}\right)-\frac{v}{r^2}+\frac{1}{r^2}\frac{\partial^2 v}{\partial \theta^2}+\frac{2}{r^2}\frac{\partial u}{\partial \theta}+\frac{\partial^2 v}{\partial z^2}\right)$$
$$+\frac{1}{\rho_m}(\rho g_\theta) \qquad (2)$$

Equation of axial component of the momentum:

$$\frac{\partial w}{\partial t}+u\frac{\partial w}{\partial r}+\frac{v}{r}\frac{\partial w}{\partial \theta}-\frac{v^2}{r}+w\frac{\partial w}{\partial z}=-\frac{1}{\rho_m}\frac{\partial P}{\partial z}$$
$$+\nu\left(\frac{1}{r}\frac{\partial}{\partial r}\left(r\frac{\partial w}{\partial r}\right)+\frac{1}{r^2}\frac{\partial^2 w}{\partial \theta^2}+\frac{\partial^2 z}{\partial z^2}\right)$$
$$+\frac{1}{\rho_m}(\rho g_z) \qquad (3)$$

Where $\boldsymbol{u,v,w}$ are the fluid velocity components in the $(\boldsymbol{r,\theta,z})$ direction, $\boldsymbol{\rho_m}$ is the melt density, $\boldsymbol{p}$ is the pressure, $\boldsymbol{\nu}$ is the kinematic viscosity, $\boldsymbol{g_r, g_z}$ are the radial and axial accelerations due to gravity. is the thermal expansion coefficient, The temperature in a unsteady state is given by energy equation:

Energy equation:

$$\frac{\partial T}{\partial t}+u\frac{\partial T}{\partial z}+\frac{v}{r}\frac{\partial T}{\partial \theta}+w\frac{\partial T}{\partial z}=$$
$$\alpha\left[\frac{1}{r}\frac{\partial}{\partial r}\left(r\frac{\partial T}{\partial r}\right)+\frac{1}{r^2}\frac{\partial^2 T}{\partial \theta^2}+\frac{\partial^2 T}{\partial z^2}\right] \qquad (4)$$

Where $\boldsymbol{T}$ is the temperature, and $\boldsymbol{\alpha}$ is the thermal diffusivity. In this case the viscous dissipation is neglected.

Continuity equation:

$$\frac{1}{r}\frac{\partial(ru)}{\partial r}+\frac{1}{r}\frac{\partial v}{\partial \theta}+\frac{\partial w}{\partial z}=0 \qquad (5)$$

2.1.1 Presentation of the grid used

In the figure.3 we shows the mesh grid which has been used to solve numerically the above equations. The physical domain is in cylindrical coordinates was subdivided into a finite number of contiguous volumes (CV) of volume V with a number of nodes 149792 and 0.01 for time step.

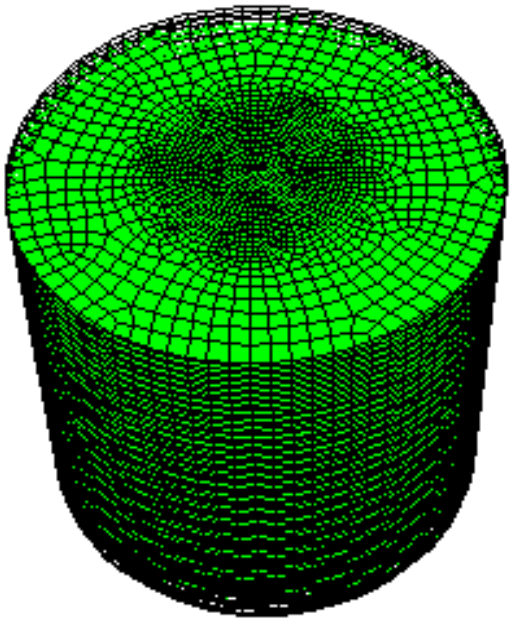

Figure 3. Three-dimensional mesh for calculation of Czochralski crucible.

Boundary conditions

The cylindrical crystal is growing from the melt in a cylindrical crucible. The crystal growth model used for numerical simulation is shown in fig. 2. It is assumed that the solute is uniformly distributed in the melt reservoir, the crucible temperature is homogeneous, the interface shape and melt free surface are planar, the interface crystal-melt is at the melting point $\boldsymbol{T_m}$. With these assumptions, we present below a description about the boundary conditions simulations for the velocity and temperature:

- At the crystal-melt interface:

$$\boldsymbol{0 \le r \le R_S\ , 0 \le \theta \le 2\pi, Z = H}$$

$$\boldsymbol{u = 0, v = R_S\omega_S = 0, w = 0}$$

$$T = T_m$$

Where ω_S is the disc rotation speed and $\boldsymbol{R_S, R_C}$ is the radius of the crystal (disc) and of the crucible respectively..

- At the melt free surface:

$$R_S \le r \le R_C\ , 0 \le \theta \le 2\pi, Z = H$$

The heat transfer from the melt free surface to the ambient is controlled by both radiation and convection according to the energy balance along the melt free surface:

$$n.k_m\vec{\nabla}T = -Bi(T - T_a) + Rad(T^4 - T_a^4)$$

Where **n** is the unit normal vector on the melt surface pointing outwards; $\mathbf{k_m}$ is the thermal conductivity of the melt. $\boldsymbol{Bi = hH/k_m}$ is the Biot number where the **h** is heat transfer coefficient . In this study the ambient temperature $\boldsymbol{T_a}$ is set to be a constant. The radiation number **Rad** is defined by:

$$\boldsymbol{Rad = \sigma\, \varepsilon_m\, (R_c - R_s) T_m{}^3 / k_m}$$

This condition is more practical when the radiative heat exchanges between the melt sapphire free surface and the surrounding surfaces such as the exposed After heater wall and crystal side surface are considered.
Where:
$\boldsymbol{\sigma}$ is the Stefan–Boltzmann constant, while $\boldsymbol{\varepsilon_m}$ is the surface emissivity of the sapphire melt and $\boldsymbol{T_m}$ the melting point of sapphire .

In the free surface, the three components of the velocity are deduced from Marangoni convection; where the tangential stress balance is required:

$$ns: t = Ma(s.\nabla T)$$

Where $\boldsymbol{s}$ is the unit tangent vector at the free surface, $\boldsymbol{t}$ is the shear stress tensor. $\boldsymbol{Ma}$ is the Marangoni number that is a measure of surface tension driven flow and is defined by:

$$Ma = \left(\frac{\partial\gamma}{\partial T}\right)(R_C - R_S)\ \Delta T/(\eta_m \alpha_m)$$

Where $\partial\gamma/\partial T$ is the surface-tension temperature coefficient, η_m the melt viscosity and ΔT is the temperature difference between the crystal-melt interface (disc) and the crucible side.

At the crucible side:

$$R = R_c\ , 0 \le Z \le H$$

The temperature at the crucible side wall, was set by the radio frequency generator.

$$T = T_m + \Delta T = T_C$$

$$u = 0, v = 0, w = R_c\omega_C = 0$$

The temperature difference ΔT between the crystal-melt interface and the crucible side is about $\Delta T \approx 45 to 50\ K$ above the melting point of sapphire ($T_m = 2323\ K$). Where T_C is the temperature of crucible equal to $2373\ K$; it is the value that is used experimentally to heat the crucible [21].

At the crucible bottom:

$$-R_c \le r \le R_c, z = 0, 0 \le \theta \le 2\pi$$

$$u = 0, v = r\omega_C = 0, w = 0$$

$$T = T_C$$

Where ω_C is the crucible rotation speed.

3. Results and discussions

The properties and growth behavior of sapphire crystals are influenced largely by the temperature distribution and convection of molten sapphire during the manufacturing process. For this raison we study the heat transfer, natural convection, effect of the Rayleigh number and Marangoni convection in the crucible Czochralski technique. We use vertical and horizontal sections to show convection phenomena that are very interesting and play an important role in the quality of the crystal produced.

3.1. Effect of the Rayleigh number (Free convection)

In this paper we study the effect of the thermal Rayleigh number Ra_T on the heat transfer and on the flow in the Czochralski crucible i-e the free convection in the growth system with non rotating crystal (seed) $(R_S\omega_S = 0)$:

Where the Rayleigh number is defined as :

$$Ra_T = Gr.Pr = \frac{g_0\beta_T\Delta T H^3}{\alpha_m \nu} = 5 \times 10^5$$

$$Gr = \frac{g_0\beta_T\Delta T H^3}{\nu^2} \quad and \quad Pr = \frac{\nu}{\alpha_m}$$

Gr is the Grashof number due to the temperature difference between the melt-crystal interface and crucible and Pr is the Prandtl number.
The numerical simulations were performed for the Al_2O_3 melt under the following conditions. The radius of the crucible is $R_c = 0.05$ m, the radius of the disc is $R_s = 0.015$ m and the height of the crucible is $H = 0.1$ m. The adimensional numbers in our case are $Ra_T = 5 \times 10^5$ and $Pr = 10.382$. The properties of sapphire (Al_2O_3) used in our simulation are presented in [21, 22, 23] and the references therein.

3.1.1 The axial temperature

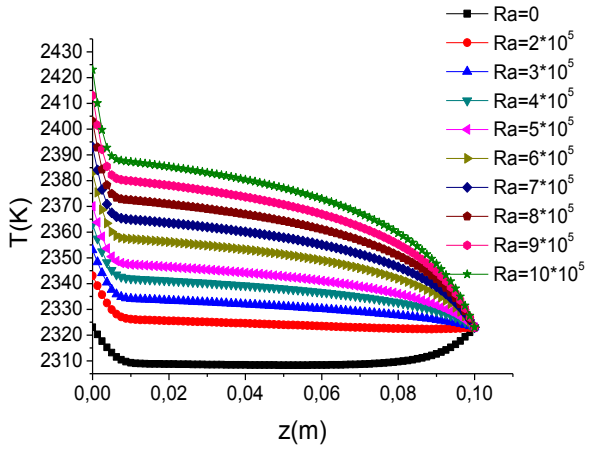

Figure 4. Axial temperature profile for different Rayleigh number.

Axial temperature profile plotted from the crucible bottom to the crystal-melt interface is shown in Figure 4. This figure indicates different axial temperature gradients which arise from heat transfer modes along the axis of symmetry of crucible. An inflection temperature is observed at the crystal-melt interface which is regarded to different temperature gradient of melt and crystal in that area. This results show the effect of the Rayleigh number $= (2 - 10) \times 10^5$; where the maximum value of temperature is $T_{max} = (2343 - 2423)\, K$ at the crucible side wall and at the crucible bottom edge. Below the melt surface the $T_{min} = 2323\, K$ at crystal-melt interface. For all the case, the maximum value of temperature difference across the melt is $\Delta T_{max}^{melt} = (47 - 100)\, K$. We notice that for low values of Ra the temperature is almost constant along the vertical axis.

3.1.2 The radial temperature

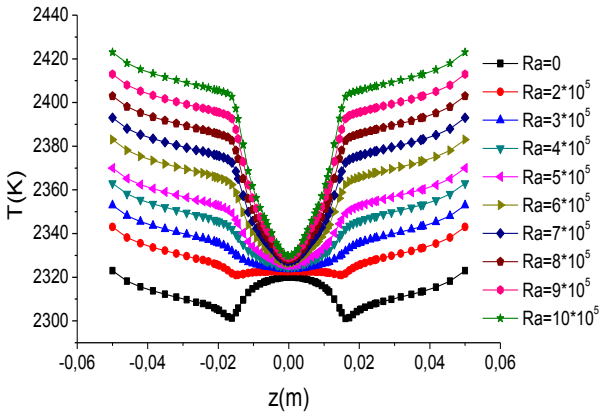

Figure 5. Temperature profile just below the melt free surface (z = 0.098 m).

Fig.5 shows the radial temperature just below the melt free surface. We notice that the radial temperature increases with increasing Rayleigh number, approaching the center of the melt - crystal interface for Rayleigh numbers greater than 3×10^5. For a Rayleigh value equal to 2×10^5 the temperature is almost constant along the interval of the melt - crystal interface. After this value we notice and the shape of the temperature profile changes from a convex shape to a concave shape. For the Rayleigh value equal to 0 we notice that the shape profile changes from a concave shape as well shown in Fig.5 with black color.

3.2. Contour and profile of velocity

3.2.1 Profile of radial velocity

In this part, we present the radial, axial, tangential and magnitude velocity profiles 2 mm under the sapphire melt free surface (z = 0.098 m).

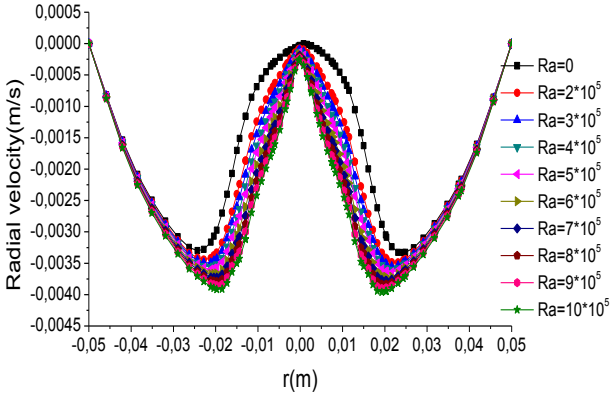

Figure 6. Radial velocity profile just below the melt free surface (z = 0.098 m).

The negative signal of the values of the radial velocity shown in figure 6 does not show that the radial velocity is negative but that the direction of the velocity is in the opposite direction. According to these curves we observe that there is symmetry in the radial flow; on the other hand we notice that the radial velocity of the fluid particles increases when the heating temperature of the crucible increases (number of Rayleigh increases).
For zero Rayleigh's number, it is clear that the values of the radial velocity are relatively higher that the other values of the Rayleigh number.

3.2.2 Profile of axial velocity

Fig. 7 shows the axial velocity profile at 2 mm just below the free surface (z = 0.098 m). We notice that there is symmetry of the axial flow in the crucible. The axial velocity of the fluid particles increases and takes a maximum value just close to the center of the crucible exactly at the two boundaries of the liquid-solid interface (-

0.015 m and 0.015 m). In the center of the crucible and along its vertical axis (from -0.015 m to 0.015 m), we notice that the axial velocity decreases and forms different trajectories (concave and convex); where the symmetry always is conserved.

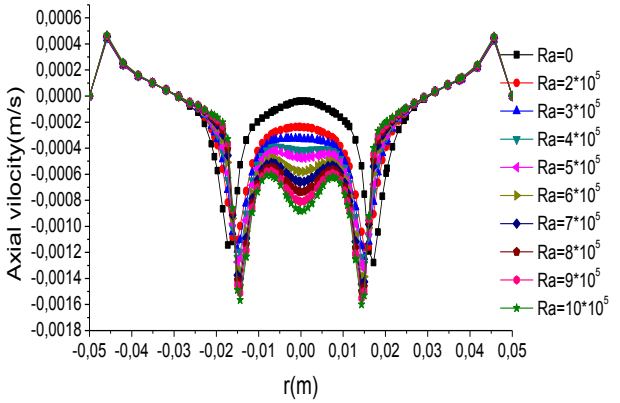

Figure 7. Axial velocity profile just below the melt free surface (z=0.098m).

3.2.3 Profile of tangential velocity

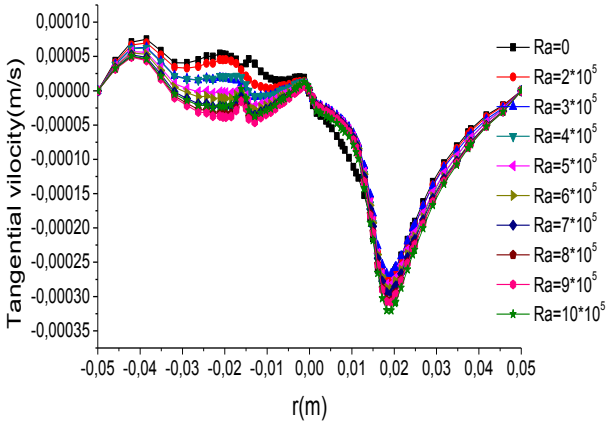

Figure 8. Tangential velocity profile just below the melt free surface (z=0.098m).

From this figure we notice, that there is no symmetry of the tangential velocity profiles relative to the symmetry axis of the crucible. We know that causes the defects in the produced crystal but when the tangential velocity takes a high values. In our case as shown in figure The non-symmetry indicates that the flow in the crucible begins to take a relatively three-dimensional form but it does not appear clearly in the contours because the values of the tangential velocity are very small (almost null). It shows the importance of the representation of profiles in this case to properly analyze what happens inside the crucible.

3.2.4 Contour and profile of velocity magnitude

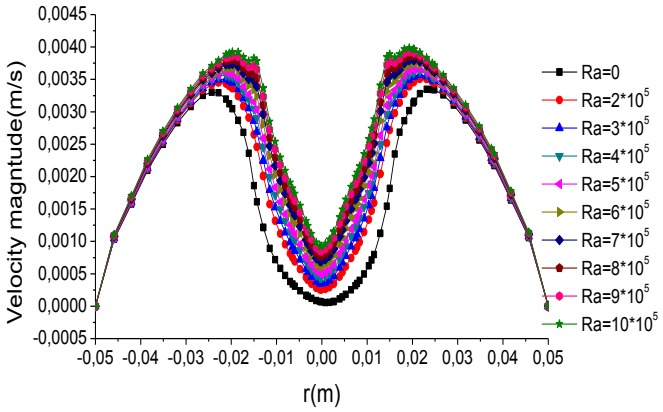

Figure 9. Velocity magnitude profile 2 mm under the melt free surface (z = 0.098 m).

Velocity magnitude is presented in fig .9 It is clear that the velocity of the fluid particles is maximal at the symmetry axis of the crucible, this results confirmed by the contour of velocity magnitude.

3.2.5 Contours of velocity

In the figure below we present the contours of velocity in the Czochralski crucible. According these results, it is noted that the flow of the fluid is two-dimensional in the plane (r, z) because of the tangential velocity which is almost null as shown in Fig 10: (d).

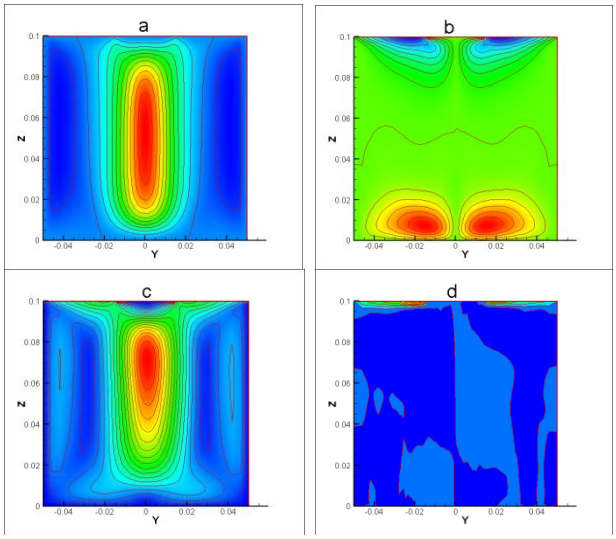

Figure 10. Presentation of the contours of velocities: (a): axial velocity; (b): radial velocity; (c): velocity magnitude; (d): tangential velocity.

It is clear that the velocity of the fluid particles is maximal at the symmetry axis of the crucible as it is

presented by the red color in the contour of velocity magnitude Fig 10: (c). In this case the axial flow is dominant in relation to the radial flow.

In the lower part of the crucible, the contour of the radial velocity indicates the presence of two contrarotating cells expressing natural convection (red color, fig10: (b)).

In the contour of radial velocity, at the upper part of the crucible, we clearly see the thermocapillary effect represented by the two convection cells (Marangoni convection) which are induced by the gradients of surface tensions. These two cells are well presented in the radial profile velocity Fig 6 by the tow maximum values of this velocity.

Tangential velocity is almost null that is showing in the contour (d) with green color, this keeps the flow two-dimensional in the crucible. The problem of the free convection in the Cz process is the high value of temperature fluctuations as showing in figs.12 and 13.

4. Illustration of unsteady state heat Transfer in the Czochralski crucible.

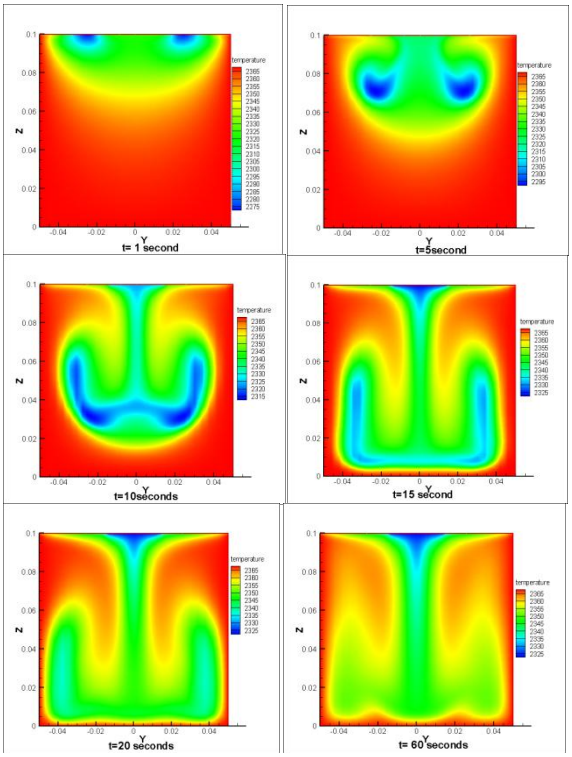

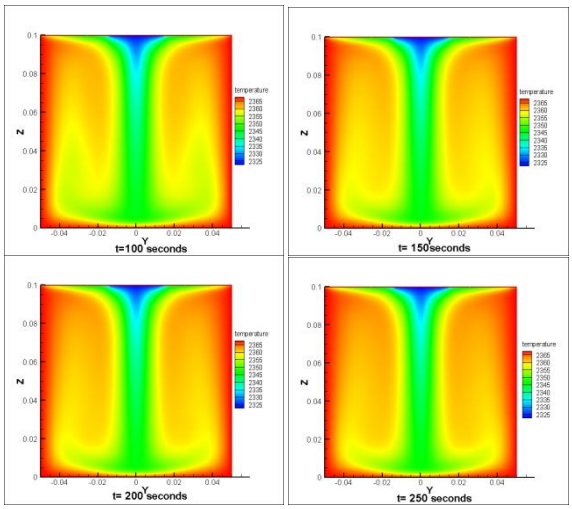

Figure 11. Heat transfer in the Cz crucible (Unsteady state).

According to these results, we notice that after a growth time equal to 150 s the steady state is reached. The contour of the temperature in the unsteady state (from 10 s) indicates a cold jet descending from the liquid solid interface through the axis of symmetry of the crucible. We also notice that at the top of the crucible there is an inclination of the isotherms near the side wall which indicates the presence of the Marangoni convection induced by the gradients of surface tensions.

We now that there are flows that begin in a aleatory way (non-symmetrical), after a certain growth time the flow takes a symmetry form in the crucible. In the case of sapphire, we notice that from the first growth time to the steady state, the sapphire flow is symmetrical along the unsteady state.

4.1 Analysis of fluctuations temperature

In order to study the thermal instabilities just below the liquid/solid interface, temperature fluctuations are analyzed for different proposed points as showing in the fig below. This study is performed using the Fast Fourier Transform method. Our simulation was conducted taking into account the none rotating of crystal, free convection in the Cz crucible, radiative heat transfer and Marangoni convection at the sapphire melt free surface.

To located the positions which have large fluctuations, five points were taken in the plane z = 0.098 m (2 mm below the crystal-melt interface.) P0 (0, 0, 0.098), P1 (0.015, 0, 0.098), P2 (0, 0.015, 0.098), P3(-0.015, 0, 0.098), P4(0, -0.015, 0.098).

Fig.12 shows the temperature fluctuations magnitude as a function of the frequency for the five points chosen just below the melt-crystal interface.

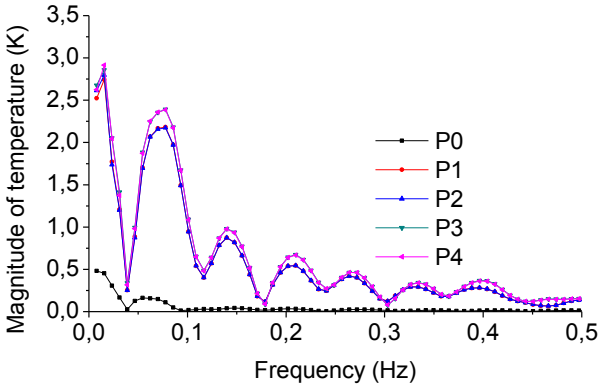

Figure 12. Temperature fluctuations at various positions just below the crystal-melt interface free convection.

According to this figure, we notice that for the point P4 the amplitude of fluctuations is higher than those found for the points P0, P1, P2 and P3. So P4 is the point adopted for our analysis.

In the next part, we have also conducted a analysis of the temperature fluctuations just near this interface for different proposed Rayleigh number using Fast Fourier Transform (FFT). The results obtained are presented in Fig.13.

For the first lower frequency, it is noted that the magnitude spectrum increases with the increase of the Rayleigh number. Between the both values 0.05 and 0.1 Hz we notice that the magnitude of temperature increases with the increase of Ra number except for Rayleigh = 5E5. In this case that corresponds to $\Delta T = 50\ K$ the magnitude take the lower value as showing in the below figure. After the frequency value 0.1 Hz, it is clear that the magnitude spectrum does not depend on the Rayleigh number in a simple way.

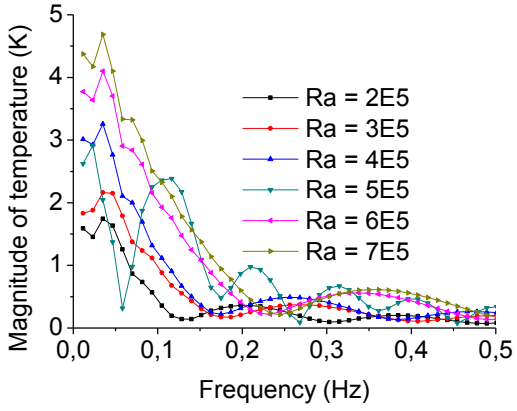

Figure 13. Magnitude of temperature fluctuations in the P4 position for various Rayleigh number.

In this case, we can say that the temperature suitable for heating the crucible is $T_{cru} = T_m + \Delta T$, i.e. d $T_{cru} = 2323\ K + 50\ K = 2373\ K$. This value of heating temperature is the temperature used experimentally to heat the crucible [21].

The displayed Fig.14 shows the maximum of magnitude of temperature fluctuations in the P4 position as a function of Rayleigh number.

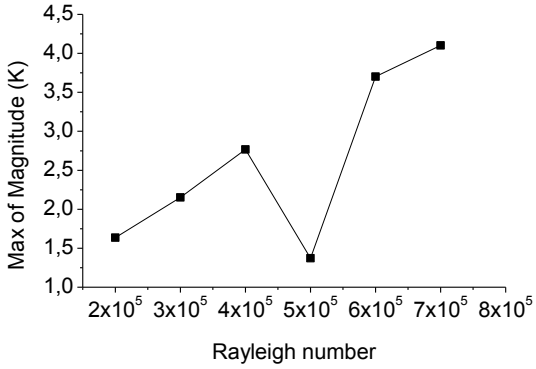

Figure 14. Magnitude of the temperature fluctuations as a function of the Rayleigh number for sapphire material.

We notice that the maximum of the fluctuations increases with the increase of Rayleigh number up to the value 4E5. For Rayleigh number = 5E5 It is noted that the magnitude has a minimum value and then come back to grow again as shown in the figure above. This result confirms our interpretation of the fig.13.

4.2 Steady state heat transfer in the crucible

Fig.15 shows the isotherms and the heat transfer in the Cz crucible of the steady state. In this part we touch on problem of free convection.

According to the figure below, we notice that the contour of the temperature indicates a cold jet (blue color) descending from the liquid-solid interface through the axis of symmetry of the crucible. We also notice that at the top of the crucible there is an inclination of the isotherms near the crucible lateral wall (green color). In this case the calculated temperature in the crucible is between 2324 K (near the sapphire melting temperature) and 2365 K near the crucible lateral wall as shown in the temperature isotherms. This inclination of the isotherms indicates the presence of the Marangoni convection induced by the gradients of surface tensions.

The shape of the melt-crystal interface is not flat as shown by the first isotherm in the figure above, although the symmetry of the heat transfer that translates the symmetry of the flow in crucible.

The melt-crystal interface shape is very important since it shows that drawing conditions are very stable; when it is flat we obtain a good quality of the pulled crystal. The convex or concave shape of melt –crystal interface is mainly induced by natural convection and temperature fluctuations.

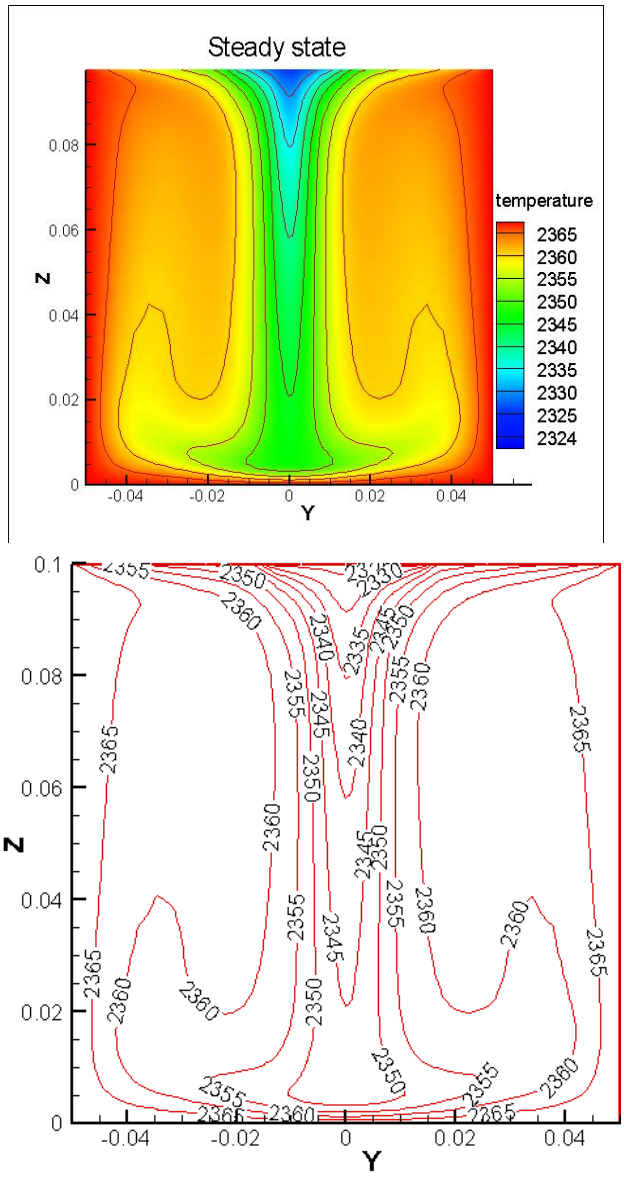

Figure 15. Isotherms and heat transfer contour in the steady state for the sapphire material $Ra = 5 \times 10^5$

4.3 Forced convection

The solution that has taken experimentally is to introduce an opposite force to the force of free convection in the opposite direction. This procedure is done either by the rotation of the crystal, or by the rotation of the fluid which is inside the crucible. In our simulation we show the effect of forced convection by introducing the rotation of crystal. To show that the forced convection (crystal speed rotation) decreases the temperature fluctuations just below the liquid-solid interface, we see the difference between the two (Free and forced convection).

According to this figure we notice that the magnitude of the temperature fluctuations in the case of free convection (0 rpm) is higher than the fluctuations in the case of forced convection (8 rpm: round per minute).

We conclude that the rotation of the crystal decrease the temperature fluctuations which gives us a good quality

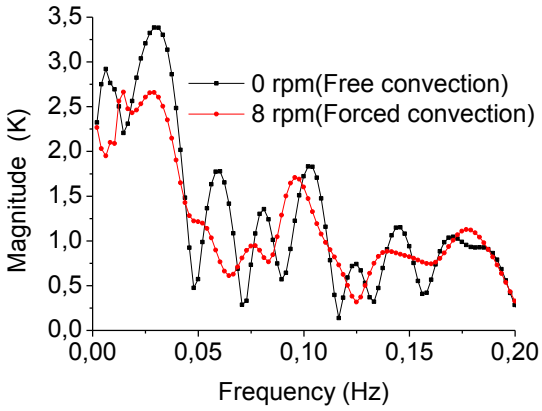

Figure 16. Fast Fourier transforms of the temperature fluctuations at P4 for free and forced convection.

of the drawn crystal. This rotation decreases the fluctuations which gives us a good quality of the crystal drawn on the other side the rotating of crystal composes a cylindrical shape which will be used in different applications.

5. Conclusion

We have performed a three-dimensional numerical investigation in order to study the effect of Rayleigh number on the natural convection in the Cz crucible and on the thermal instabilities. The heat transfer, melt natural convection, temperature fluctuations, radiative heat transfer and Marangoni convection, were conducted for Al_2O_3 melt. We used the Fast Fourier Transform method for study the temperature fluctuations just below the melt-crystal interface. Our objective is to reduce the fluctuations of temperature near the interface by taking into account the case of non-rotating seed. This study shows that

The unsteady state flow in the Czochralski crucible remains axisymmetric to the first growth time up to the steady state. It is due to the homogeneous horizontal and vertical temperature gradient.

The heating of the crucible walls up about to 2423 K ($Ra = 10^6$) does not change the symmetry of flow in the crucible but it augments the temperature fluctuations and creates large cells of the marangoni convection which depends directly on the gradient of the temperature.

The melt –crystal interface shape is mainly induced by natural convection and temperature fluctuations in the Czochralski process.

In the absence of crystal rotation, the flow attains a steady state even for higher value for Rayleigh numbers but in this case the instabilities of temperature increase in the Czochralski system.

As the Rayleigh number increases, multiple frequency oscillations with varying amplitudes are observed.

The maximum of magnitude of temperature fluctuations increases with the increasing of the Ra number except the value that has a minimum frequency. This lower magnitude temperature corresponds to the heating temperature of crucible used experimentally.

The melt natural convection cannot be eliminated and is strongly influenced by temperature distribution along the crucible wall.

To obtain a high quality sapphire single crystal, the melt natural convection must be controlled in the crucible by introduce the forced convection (due to the crystal and crucible rotation and electromagnetically induced convection if the electromagnetic field).

References

[1] Thierry Duffar. Crystal Growth Processes Based on Capillarity. Czochralski, Floating Zone, Shaping and Crucible Techniques. © 2010 John Wiley & Sons Ltd.

[2] Fukuda T., Shaped Crystals, Growth by Micro-Pulling- Down Technique .Advances IN materials Research 8, 2007.

[3] Chandra P. Khattak, Frederick Schmid, Growth of the world's largest sapphire crystals, Journal of Crystal Growth. (2001)225.

[4] Y. G. Son, J.H. Ryu, W. J. Lee, Y. C. Lee, H. H. Jo and Y. H. Park. Numerical study of three-dimensional convection due to buoyancy force in an aluminum oxide melt for Kyropoulos growth,. Journal of Ceramic Processing Research. Vol. 16, No. 1, (2015)68-73

[5] N. Kobayashi, "Computational simulation of the melt flow during Czochralski growth," Journal of Crystal Growth, vol. 43, no. 3, (1978)357–363

[6] N. Kobayashi, "Hydrodynamics in Czochralski growth-computer analysis and experiments," Journal of Crystal Growth, vol. 52, (1981)425–434,

[7] J. Derby, L. Atherton, and P. Gresho, "An integrated process model for the growth of oxide crystals by the Czochralski method," Journal of crystal growth, vol. 97, no. 3, (1989)792–826

[8] C. Jing, N. Imaishi, T. Sato, and Y. Miyazawa, "Three-dimensional numerical simulation of oxide melt flow in Czochralski configuration," Journal of crystal growth, vol. 216, no. 1, (2000)372–388,

[9] M. H. Tavakoli and H. Wilke, "Numerical study of heat transport and fluid flow of melt and gas during the seeding process of sapphire Czochralski crystal growth," Crystal growth & design, vol. 7, no. 4, (2007)644–651

[10] M. Tavakoli and H. Wilke, "Numerical investigation of heat transport and fluid flow during the seeding process of oxide Czochralski crystal growth part 1: non-rotating seed," Crystal Research and Technology, vol. 42, no. 6, (2007)544–557

[11] J. Banerjee and K. Muralidhar, "Simulation of transport processes during Czochralski growth of yag crystals," Journal of crystal growth, vol. 286, no. 2, (2006)350–364

[12] C. Brandle, "Flow transitions in Czochralski oxide melts," Journal of Crystal Growth, vol. 57, no. 1, (1982)65–70

[13] H. Kimura, "Flow transitions in simulated Czochralski method with tetradecane (c14h30) instead of bi12sio20," Journal of crystal growth, vol. 78, no. 1, (1986)19–23

[14] H. Kimura, "Growth instability in simulations of the Czochralski method with tetradecane and water," Journal of crystal growth, vol. 78, no. 2, (1986)322–324

[15] Hirata, M. Tachibana, Y. Okano, and T. Fukuda, "Observation of crystal-melt interface shape in simulated Czochralski method with model fluid," Journal of crystal growth, vol. 128, no. 1, (1993)195–200

[16] Z. Galazka and H. Wilke, "Heat transfer and fluid flow during growth of y3al5o12 single crystals using the Czochralski method," Crystal Research and Technology, vol. 35, no. 11-12, (2000)1263–1278

[17] Z. Gałazka and H. Wilke, "Influence of marangoni convection on the flow pattern in the melt during growth of y3al5o12 single crystals by the Czochralski method," Journal of crystal growth, vol. 216, no. 1, (2000)389–398

[18] M. Tavakoli, H. Wilke, and N. Crnogorac, "Influence of the crucible bottom shape on the heat transport and fluid flow during the seeding process of oxide Czochralski crystal growth," Crystal Research and Technology, vol. 42, no. 12, (2007)1252–1258

[19] Q. Xiao and J. J. Derby, "Heat transfer and interface inversion during the Czochralski growth of yttrium aluminum garnet and gadolinium gallium garnet," Journal of Crystal Growth, vol. 139, no. 1, (1994)147–157

[20] M. Kobayashi, T. Hagino, T. Tsukada, and M. Hozawa, "Effect of internal radiative heat transfer on interface inversion in Czochralski crystal growth of oxides," Journal of crystal growth, vol. 235, no. 1, (2002)258–270

[21] A. Nehari. Etude et caractérisation de la synthèse de milli-billes d'alumine alpha et de la cristallogenèse du saphir pur et dopé titane (Ti^{3+}). Ph.D. Thesis. University of Lyon. France (2011).

[22] H. Azoui, A. Laidoune, D. Haddad, D. Bahloul, and F. Merrouchi. " Numerical simulation of the crystal growth of Ti:Al_2O_3 material by the µ-PD Technology". J. of New Technol. Mater. Vol. 06, N°02 . (2016)102-110

[23] A. Laidoune. « Croissance des fibres cristallines pour usage dans l'optoélectronique ». Thèse de doctorat. Université de Batna1, Algeria (2010).